

A Robust Multichannel Lung Sound Recording Device

Elmar Messner¹, Martin Hagmüller¹, Paul Swatek² and Franz Pernkopf¹

¹Signal Processing and Speech Communication Laboratory, Graz University of Technology, Graz, Austria

²Division of Thoracic and Hyperbaric Surgery, Medical University of Graz, Graz, Austria

Keywords: Lung Sounds, Lung Sound Transducer, Air-Coupled Microphone, Multichannel Recording Device, Sound Classification.

Abstract: This paper presents a robust multichannel lung sound recording device (LSRD) for automatic lung sound classification. Compared to common approaches, we improved the usability and the robustness against body sounds and ambient noise. We developed a novel lung sound transducer (LST) and an appropriate attachment method realized as a foam pad. For analogue prefiltering, preamplification, and digitization of the lung sound signal, we use a composition of low-cost standard audio recording equipment. Furthermore, we developed a suitable recording software. In our experiments, we show the robustness of our LSRD against ambient noise, and we demonstrate the achieved signal quality. The LST's microphone features a signal-to-noise ratio of $SNR = 80$ dB. Therefore, we obtain a bandwidth of up to a frequency of $f \approx 2500$ Hz for vesicular lung sound recordings. Compared to the attachment of the LST with self-adhesive tape, the foam pad achieves an attenuation of ambient noise of up to 50 dB in the relevant frequency range. The result of this work is a multichannel recording device, which enables a fast gathering of valuable lung sounds in noisy clinical environments without impeding the daily routines.

1 INTRODUCTION

Computer-aided lung sound analysis offers advantages for medical diagnosis, such as digital storage, monitoring in critical care settings, computer-supported analysis, and comparison among different sound recordings. Despite these advantages, it is far away from being used in clinical settings. One reason is the lack of efficiency and performance due to the variability in the recordings (Reichert et al., 2008; Gurung et al., 2011). Recently, lung sound research mainly focused on the classification task. Researchers either performed lung sound recordings independently or used appropriate databases in their experiments (Palaniappan et al., 2013). Sensors applied to lung sound recording are air-coupled microphones, contact sensors and modified stethoscope chest pieces (Pasterkamp et al., 1993; Kraman et al., 2006). The most common recording technique employs air-coupled microphones attached with self-adhesive tape. This approach lacks of sensitivity against body sounds and ambient noise (Zanartu et al., 2009; Pasterkamp et al., 1999; Liu et al., 2013). Moreover, for multichannel usage the attachment of several lung sound transducers (LSTs) with self-adhesive tape results in a poor usability and increases

the sensitivity against measurement errors.

In this paper, we introduce a robust lung sound recording device (LSRD) to circumvent the aforementioned drawbacks. It supports a reliable recording of a high quality lung sound database for multichannel lung sound classification. To obtain clean lung sound recordings, we focused on the recording stage and reduced post-processing. Furthermore, it was important that the LSRD is suitable to record lung sounds for a large number of diseases. This is reflected in the distribution and position of the LSTs. Beside distinct adventitious lung sounds (Sovijarvi et al., 2000), it should reliably allow the estimate of changes in amplitude of lung sounds, which is necessary for the detection of, e.g., pneumothorax (Hayashi, 2011).

Based on the approach with air-coupled microphones (Pasterkamp et al., 1993), we developed a novel lung sound transducer ensuring a high signal quality. For the attachment of the LSTs, we designed a foam pad similar to the Stethographics STG 16 (Murphy, 2007). It records lung sounds in supine position. We implemented the analog prefiltering, preamplification, and digitization of the lung sound signal with a composition of standard audio recording equipment. The entire LSRD consists of the foam

pad (our so called auscultation pad) and a pneumotachograph, both working with an appropriate recording software on a personal computer.

We organized the paper as follows. Section 2 presents our LST design and the auscultation pad. Section 3 gives an overview on the remaining components of the LSRD. The achieved signal quality and the robustness against ambient noise is treated in Section 4. Section 5 describes the measurement procedure and Section 6 concludes the paper.

2 AUSCULTATION PAD

The core of our LSRD is the auscultation pad. It is a foam pad with 16 LSTs distributed on its surface. We adapted our LST design for this attachment method. In the following subsections, we separately describe the LST design and the foam pad.

2.1 Lung Sound Transducer

We developed a novel LST according to the approach with air-coupled electret-condenser microphones (Pasterkamp et al., 1993). Figure 1 shows our final LST. We use a Littmann Classic II chest piece as coupler. We inserted an electret-condenser microphone capsule (ECMC) in such a way that the stethoscope chest piece is acting as a conical coupler between the microphone capsule and the human skin. The depth of the conical coupler is $d = 2.2$ mm, and the width is $w = 33$ mm. Its shape corresponds to the recommendations in (Wodicka et al., 1994; Kraman et al., 1995). We used the diaphragm of the chest piece to cover its opening. It prevents the filling of the coupler cavity with skin, and, thus, it ensures its acoustic effect. This is important for varying contact pressure, and, therefore, it is relevant for our attachment method discussed in Section 2.2. The diaphragm further enables a convenient disinfection of the LST, and it protects the ECMC from scratching

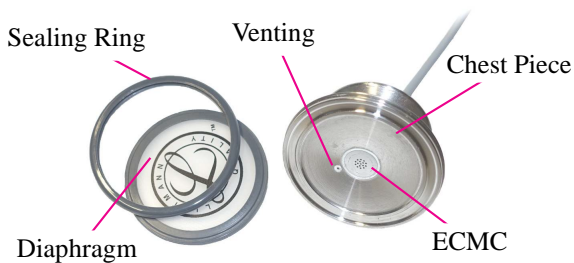


Figure 1: Lung sound transducer consisting of an electret-condenser microphone capsule (ECMC) inserted in a Littmann Classic II chest piece.

body hair and dirt.

To allow static pressure equalization between the coupler chamber and the surrounding air, we inserted a small vent into the chest piece. We used a thin-wall 23-g needle with a length of $l = 11.5$ mm and with an inner diameter of $d = 0.35$ mm, according to the recommendations in (Kraman et al., 1995). As ECMC, we used the Primo EM172, which features a very high signal-to-noise ratio of $SNR = 80$ dB and a sensitivity of -27 dB (re $1V/Pa$). These specifications are distinctly better than those of widely used microphones, like the Sony ECM-44BPT (Sen and Kahya, 2006) or the Sony ECM-77B (Dokur, 2009), which feature an $SNR \leq 64$ dB.

2.2 Pad

The attachment of the LST is a crucial part, because of its high sensitivity against air- and tissue-borne sounds (Zanartu et al., 2009; Pasterkamp et al., 1999). Therefore, we developed a foam pad, the auscultation pad shown in Figure 2. It consists of several foam lay-



Figure 2: Arrangement of the lung sound transducers on the auscultation pad. The center line represents the spine.

ers and a cover of artificial leather. The topmost layers hold the LSTs. There is a small cavity beneath each LST, which avoids increasing contact pressure due to the underlying foam. Furthermore, the cavity prevents the foam from touching the venting of the LST or even clogging it. By using different kinds of foam, we designed a shape that adapts to almost every physique. This construction provides a symmetric contact pressure with respect to the spine. We ar-

ranged the LSTs on the surface of the auscultation pad with a fixed pattern, which almost matches the one proposed in (Sen and Kahya, 2006). The pad enables a fast attachment of the LST on the posterior chest by simply placing the auscultation pad under the back of the patient in supine position. To further stabilize the patient, we extended the auscultation pad with two additional pads, one for the head and another one for the buttocks, as shown in Figure 3. We are able to achieve a high robustness against body sounds and ambient noise with an overall high lung sound signal quality. Further details are presented in Section 4. The attenuation of ambient noise is due to the surrounding foam. We achieve the robustness against body sounds due to the reliable attachment and almost no movement of the back during breathing in the supine position. The surrounding foam further prevents the interspersal of body-borne noise in the LST cable. Another advantage is the balanced audio connection from the auscultation pad to the microphone preamplifiers, which reduces the susceptibility to external noise.

3 REMAINING SETUP COMPONENTS

We use the auscultation pad as part of a mobile recording setup (Figure 3). The setup consists of an equipment cart, which includes the recording hardware, two screens, a pneumotachograph, and the pads. The following subsections contain some details about the remaining components.

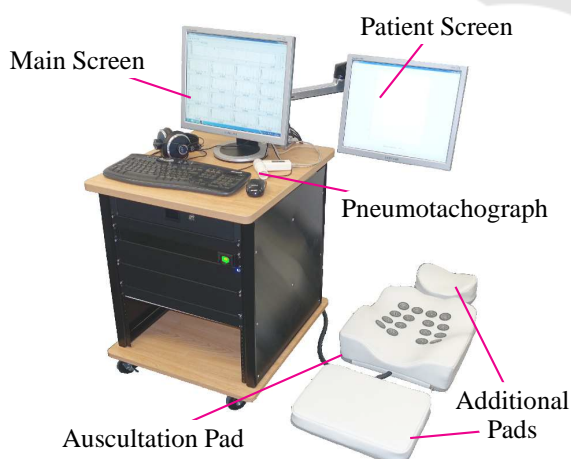


Figure 3: Mobile lung sound recording device containing the auscultation pad and the remaining components.

3.1 Recording Hardware

We implemented the analogue prefiltering, preamplification, and digitization of the lung sound signal with low-cost standard audio recording equipment. The composition of the appropriate hardware fulfills the requirements of the CORSA guidelines (Vannuccini et al., 2000).

We use two SM Pro Audio EP84 8-channel microphone preamplifiers with the integrated ADAT interface SM Pro Audio PR8IIA. Beside the high-pass filtering (cutoff frequency $f_c = 80$ Hz, with a slope of 18 dB/oct), the preamplification, and the analog-to-digital conversion of the LST signal, the SM Pro Audio PR8IIA provides the supply voltage (phantom power) for the ECMCs. For the appropriate operating voltage of the ECMCs, we further use AKG MPA VL phantom power adapters. They convert the phantom power of 48V to the required 3V~10V. The AKG MPA VL phantom power adapter features a high-pass characteristic with a cutoff frequency of $f_c = 80$ Hz and a slope of 6 dB/oct. In a series-connection with the microphone preamplifier, an overall high-pass characteristic with a slope of 24 dB/oct is achieved. The high-pass filters of the microphone preamplifiers and the phantom power adapters are implemented as Bessel filters. Therefore, they feature an approximately linear phase response. The two SM Pro Audio EP84 are connected with an RME Fireface 800 audio interface. This represents a firewire multichannel audio recording device for a computer. For the lung sound recordings we use a sampling frequency of $f_s = 16$ kHz and a resolution of 24 Bit.

3.2 Pneumotachograph

The simultaneous recording of the velocity of respired air and the lung sounds makes the distinction between inspiratory and expiratory phases possible. Furthermore, we almost reach a uniform lung sound signal intensity profile by specifying the respiratory behavior of the patient, resulting in a high quality database. We use a Schiller SP 260 pneumotachograph connected via the USB port.

3.3 Recording Software

We developed a MATLAB GUI for the simultaneous recording of the air flow and the lung sounds. Beside the recording task, it enables the gathering of meta-data and the clinical report.

We use Playrec for the multichannel recording of the lung sound signals with MATLAB. For the lung signal, we read the serial port of the pneumotacho-



Figure 4: MATLAB GUI for the recording of the air flow and the lung sounds signals.

graph. Figure 4 shows the main screen of the software, featuring simultaneously recorded air flow and lung sounds. Furthermore, we have a patient screen to display the measured air flow in real time.

4 ROBUSTNESS AND SIGNAL QUALITY

In this section, we show the achieved signal quality by means of the SNR and the frequency range of the recording setup. We further demonstrate the robustness against ambient noise with a simple experiment.

4.1 Robustness Against Ambient Noise

The CORSA guidelines (Rossi et al., 2000) recommend to have environmental condition with a background noise level of preferably < 45 dB(A) during lung sound recordings. These requirements are not always given in clinical setting.

We compared the performance of our auscultation pad in a noisy setting with the attachment-method of the LST with self-adhesive tape (Pasterkamp et al., 1993). The experiment took place in a small room. We considered two measurement scenarios. In the first scenario we centered the auscultation pad on the floor with a test person lying on it. In the second scenario, we placed a chair in the center of the room, with the test person in a sitting position.

With self-adhesive tape, we attach an LST on the persons posterior chest, at the same position where it was attached with the auscultation pad. The residual signal acquisition chain remained the same for both scenarios, as introduced in Section 3. As noise

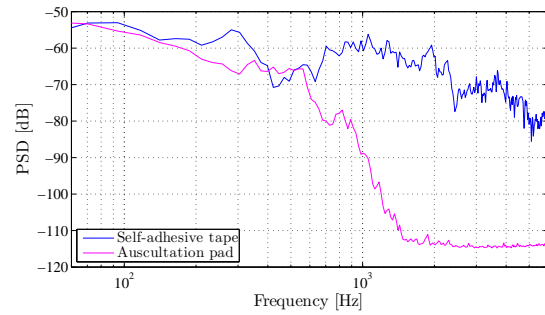


Figure 5: Attenuation of background noise of the auscultation pad compared to the attachment method of lung sound transducers with self adhesive tape.

sources, we used five loudspeakers, which played back white Gaussian noise. The loudspeakers feature a flat frequency response from $f = 80$ Hz to $f = 20$ kHz. We measured the A-weighted equivalent sound level for both scenarios at the position of the sensor over 30 seconds with $L_{Aeq} = 68$ dB. During the recording of the LST signal, we instructed the test person to hold its breath for 15 seconds and played back the white Gaussian noise.

Figure 5 shows the power spectral density (PSD) for the LST signal in both scenarios in the relevant frequency range. We see a distinct attenuation compared to the attachment with self-adhesive tape, starting above a frequency of $f = 500$ Hz. At a frequency of $f \approx 2$ kHz the difference is up to 50 dB.

4.2 Signal Quality

In Figure 6 we show the SNR of our recording setup by illustrating the spectral characteristics of the vesicular lung sound of a healthy adult person. The blue line shows the spectral characteristics during the inspiratory phase. The red line shows the background noise recorded at breath hold; the frequency components in the low-frequency range are mainly caused by body sounds.

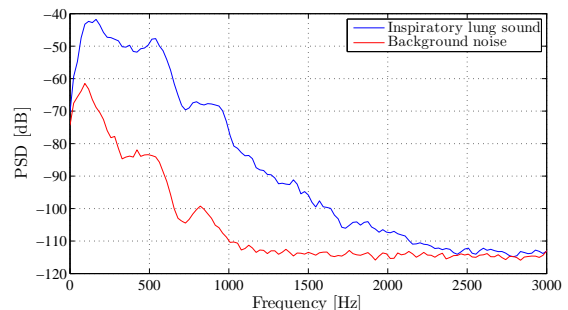


Figure 6: Spectral characteristics of normal breath sounds and background noise at breath hold, recorded at the posterior chest of a healthy adult.

We achieve a signal-to-noise ratio of up to $SNR = 75$ dB with an additional head room of around 5 dB. Due to the high SNR value, we reach a bandwidth up to a frequency of $f \approx 2500$ Hz.

5 MEASUREMENT PROCEDURE

The lung sounds are recorded in the supine position on an examination table. The auscultation pad is placed under the back of the patient. For the orientation of the patient on the pad, we use a defined distance between the the 7th cervical (C7) vertebra and the topmost row of sensors. The patient is instructed to lie quietly on the table and to breath with a maximum inspiratory flow of 1.5 l/s. This corresponds to values used from the authors in (Jones et al., 1999; Malmberg et al., 1995) and also the recommendations in the CORSA standard (Vannuccini et al., 2000). The recording time can be specified in the recording software.

6 CONCLUSIONS

We developed a robust lung sound recording device (LSRD), which reliably records a high quality lung sound database for multichannel lung sound classification. With preliminary measurements, we successfully underline the robustness of our newly designed auscultation pad with respect to ambient noise. Compared to the attachment of the LST with self-adhesive tape, we achieve an attenuation of ambient noise of up to 50 dB in the relevant frequency range. Due to the high signal-to-noise ratio of our LST's microphone of $SNR = 80$ dB, we obtain a bandwidth of up to $f = 2500$ Hz for vesicular lung sounds. For carefully performed measurements, our LSRD reduces the post-processing to band-pass filtering and heart sound reduction.

As future work, we plan to record a lung sound database for several lung diseases. Furthermore, we will focus on the classification of lung sounds.

ACKNOWLEDGEMENTS

This project was supported by the government of Styria, Austria, under the project call HTI:Tech_for_Med. The authors acknowledge 3M™ for providing Littmann® stethoscope chest pieces and Schiller AG for the support with a spirometry solution.

REFERENCES

- Dokur, Z. (2009). Respiratory sound classification by using an incremental supervised neural network. *Pattern Analysis and Applications*, 12(4):309–319.
- Gurung, A., Scrafford, C. G., Tielsch, J. M., Levine, O. S., and Checkley, W. (2011). Computerized lung sound analysis as diagnostic aid for the detection of abnormal lung sounds: a systematic review and meta-analysis. *Respiratory medicine*, 105(9):1396–1403.
- Hayashi, N. (2011). Detection of pneumothorax visualized by computer analysis of bilateral respiratory sounds. *Yonago acta medica*, 54(4):75.
- Jones, A., Jones, R. D., Kwong, K., and Burns, Y. (1999). Effect of positioning on recorded lung sound intensities in subjects without pulmonary dysfunction. *Physical Therapy*, 79(7):682–690.
- Kraman, S. S., Wodicka, G. R., Oh, Y., and Pasterkamp, H. (1995). Measurement of respiratory acoustic signals. Effect of microphone air cavity width, shape, and venting. *CHEST Journal*, 108(4):1004–1008.
- Kraman, S. S., Wodicka, G. R., Pressler, G. A., and Pasterkamp, H. (2006). Comparison of lung sound transducers using a bioacoustic transducer testing system. *Journal of Applied Physiology*, 101(2):469–476.
- Liu, S., Gao, R. X., John, D., Staudenmayer, J., and Freedson, P. (2013). Tissue artifact removal from respiratory signals based on empirical mode decomposition. *Annals of biomedical engineering*, 41(5):1003–1015.
- Malmberg, L. P., Pesu, L., and Sovijärvi, A. (1995). Significant differences in flow standardised breath sound spectra in patients with chronic obstructive pulmonary disease, stable asthma, and healthy lungs. *Thorax*, 50(12):1285–1291.
- Murphy, R. (2007). Development of acoustic instruments for diagnosis and management of medical conditions. *Engineering in Medicine and Biology Magazine, IEEE*, 26(1):16–19.
- Palaniappan, R., Sundaraj, K., and Ahamed, N. U. (2013). Machine learning in lung sound analysis: a systematic review. *Biocybernetics and Biomedical Engineering*, 33(3):129–135.
- Pasterkamp, H., Kraman, S., DeFrain, P., and Wodicka, G. (1993). Measurement of respiratory acoustical signals. Comparison of sensors. *CHEST Journal*, 104(5):1518–1525.
- Pasterkamp, H., Wodicka, G., and Kraman, S. (1999). Effect of ambient respiratory noise on the measurement of lung sounds. *Medical & Biological Engineering & Computing*, 37(4):461–465.
- Reichert, S., Gass, R., Brandt, C., and Andrès, E. (2008). Analysis of respiratory sounds: state of the art. *Clinical medicine. Circulatory, respiratory and pulmonary medicine*, 2:45.
- Rossi, M., Sovijärvi, A., Piirila, P., Vannuccini, L., Dalmaso, F., and Vanderschoot, J. (2000). Environmental and subject conditions and breathing manoeuvres for respiratory sound recordings. *European Respiratory Review*, 10(77):611–615.

- Sen, I. and Kahya, Y. (2006). A multi-channel device for respiratory sound data acquisition and transient detection. In *Proceedings of the 27th Annual International Conference of the IEEE Engineering in Medicine and Biology Society (EMBS'06)*, pages 6658–6661.
- Sovijarvi, A., Malmberg, L., Charbonneau, G., Vanderschoot, J., Dalmaso, F., Sacco, C., Rossi, M., and Earis, J. (2000). Characteristics of breath sounds and adventitious respiratory sounds. *European Respiratory Review*, 10(77):591–596.
- Vannuccini, L., Earis, J., Helisto, P., Cheetham, B., Rossi, M., Sovijarvi, A., and Vanderschoot, J. (2000). Capturing and preprocessing of respiratory sounds. *European Respiratory Review*, 10(77):616–620.
- Wodicka, G. R., Kraman, S. S., Zenk, G. M., and Pasterkamp, H. (1994). Measurement of respiratory acoustic signals. Effect of microphone air cavity depth. *CHEST Journal*, 106(4):1140–1144.
- Zanartu, M., Ho, J. C., Kraman, S. S., Pasterkamp, H., Huber, J. E., and Wodicka, G. R. (2009). Air-borne and tissue-borne sensitivities of bioacoustic sensors used on the skin surface. *IEEE Transactions on Biomedical Engineering*, 56(2):443–451.

